ENHANCED ETHANOL VAPOR SENSING OF SnO₂/ZnO NANOCOMPOSITE FILMS DEPOSITED BY SPRAY PYROLYSIS

Pham Van Vinh

VNU University of Engineering and Technology

ARTICLE INFO ABSTRACT 18/9/2024 This study focuses on SnO₂/ZnO composite films deposited on glass substrates Received: at 400°C using a spray pyrolysis method. The crystal structures analyzed using X-ray diffraction confirm the presence of SnO₂ and ZnO phases. The number Revised: 09/12/2024 and intensity of SnO2 diffraction peaks increase with the increase in Sn/Zn **Published:** ratios. The optical properties of ZnO, SnO₂, and SnO₂/ZnO composite films, reveal that the absorption edge of the composite films shift toward the **KEYWORDS** absorption edge of SnO₂ as the Sn/Zn ratio increases. The band gaps of SnO₂ SnO₂/ZnO and ZnO were found to be 3.94 eV and 3.25 eV, respectively. The I-V curve of Spray pyrolysis the composite films are nonlinear due to the formation of a heterojunction. Scanning electron microscopy images reveal morphological changes from Ethanol sensor hexagonal dipyramid crystals to spherical particles as the Sn/Zn ratio Adsorbs oxygen increased. Particle sizes reduces to around 10 nm at Sn/Zn ratios of 1/2. The Sensitization mechanisms sensitivity of films improves significantly with increased Sn/Zn ratios up to 1/2. The increased sensitivity is attributed to the enhanced surface morphology and smaller grain sizes. Optimal sensing performance is achieved at 250°C, where the response increased with temperature before reaching a saturation point. Higher Sn/Zn ratios improved sensor response. The films deposited with Sn/Zn ratio of 1/2 exhibit the highest sensor response.

CẢI THIÊN ĐỘ NHAY HƠI CÔN CỦA MÀNG TỔ HỢP SnO2/ZnO ĐƯỢC CHẾ TẠO BẰNG PHƯƠNG PHÁP PHUN NHIỆT PHÂN

Phạm Văn Vĩnh

Trường Đại học Công nghệ - ĐH Quốc gia Hà Nội

THONG TIN BAI BAO TOM TAT

Ngày nhận bài: Ngày hoàn thiên:

TỪ KHÓA

SnO₂/ZnO Phun nhiệt phân Cảm biến nhạy hơi cồn Oxy hấp phụ Cơ chế nhạy

18/9/2024 Nghiên cứu này tập trung vào màng composite SnO₂/ZnO phủ trên để thủy tinh bằng phương pháp phun nhiệt phân ở 400°C. Kết quả phân tích cấu trúc tinh thể đã xác nhận sự có mặt của các pha SnO₂ và ZnO. Số lượng và Ngày đăng: 09/12/2024 cường độ các đỉnh nhiễu xạ SnO2 tăng khi tỷ lệ Sn/Zn tăng. Phổ hấp thụ quang cho thấy, bờ hấp thụ của màng tổ hợp SnO2/ZnO dịch chuyển về phía gần bờ hấp thụ của SnO₂ khi tăng tỷ lệ Sn/Zn. Độ rộng vùng cấm của các màng tổ hợp SnO₂/ZnO nằm giữa ZnO (3,25 eV) và SnO₂ (3,94 eV). Đường cong I-V của màng composite không tuyến tính do sự hình thành của một lớp chuyển tiếp dị thể. Ảnh hiển vi điện tử quét cho thấy sự thay đổi hình thái hạt tinh thể từ hình lục giác dạng kim tự tháp sang các hạt hình cầu khi tỷ lệ Sn/Zn tăng. Kích thước hạt giảm xuống khoảng 10 nm ứng với tỷ lệ Sn/Zn bằng 1/2. Độ nhạy của màng được cải thiện đáng kể khi tăng tỷ lệ Sn/Zn lên đến 1/2. Điều này được cho là do hình thái bề mặt được cải thiên và kích thước hạt được thu nhỏ. Đô đáp ứng của cảm biến tăng theo nhiệt độ cho đến nhiệt độ bão hòa và tối ưu ở 250°C. Độ đáp ứng của cảm biến tăng theo chiều tăng của tỷ lệ Sn/Zn. Màng được chế tạo với tỷ lệ Sn/Zn bằng 1/2 cho thấy độ đáp ứng cao nhất.

DOI: https://doi.org/10.34238/tnu-jst.11139

Email: vinhpv@vnu.edu.vn

230(06): 132 - 140

1. Introduction

In the context of technological development and increasing safety demands, monitoring and controlling ethanol vapor concentrations in the air have become urgent issues in various fields, including traffic safety, healthcare, industrial production, and environmental management. Ethanol vapor sensors are crucial devices that detect and accurately measure ethanol concentrations, providing timely and appropriate warnings [1] - [5]. However, the development of sensors with high sensitivity, fast response times, and stability remains a challenge.

In recent years, metal oxide semiconductor materials have attracted significant interest in the development of gas sensors, including ethanol vapor sensors. Materials such as ZnO and SnO₂, with their unique nanostructures and electronic properties, have been widely studied due to their strong interaction with gas molecules, especially ethanol molecules [6] - [10]. Both ZnO and SnO₂ are n-type semiconductors with wide bandgaps, easy to fabricate, and capable of forming composite structures that enhance sensing properties through synergistic effect and signal amplification. When combined in a composite structure, these materials can significantly improve sensor performance, including sensitivity, selectivity, and response time [11] - [16].

Recently, composite or hybrid SnO₂/ZnO materials with special structures, such as hollow nanostructures [13], [14], [17], nanorods [12], [15], nanoflowers [18], nanowires [19] and nanotubes [20] have demonstrated excellent sensitivity to ethanol vapor. However, most of these structures are not created directly on the substrate. They are synthesized in powder form then dispersed in solvents and coated on electrodes. Although this method can easily create various special structures, it fails to produce a stable working device due to the difficulty of adhering particles to the electrode. Films prepared by this method are challenging to apply in practical applications since even minor impacts can dislodge the material layer. The film grown directly on the electrode may not have as high sensitivity as the material synthesized in nanoparticle form [6], [17], [21] – [26], but it exhibits excellent adhesion and stability, making it highly practical for real-world applications.

There are many different methods that can be used to coat the film directly on the substrate. One of them is the spray pyrolysis method. This is an efficient thin-film deposition technique that allows precise control of deposition parameters and has been used to create composite ZnO/SnO₂ thin films with unique properties [27], [28]. This method not only produces uniformly nanostructured thin films but also optimizes their properties by adjusting the composition and microstructure of the films. Additionally, spray pyrolysis offers advantages in production cost, scalability, and feasibility for the large-scale development of gas sensor devices.

This paper focuses on the deposition process of SnO₂/ZnO nanocomposite thin films using spray pyrolysis method, along with the evaluation of their structural, morphological, and ethanol vapor sensing characteristics.

2. Methodology

2.1. Deposition method

The thin films of ZnO and SnO₂/ZnO are deposited by a compress sprayer under the control of computer. The spray solution is preparad by dissolving Zn(CH₃COO)₂.2H₂O in C₂H₅OH at a molarity of 0.2M. After 60 min stirring, an appropriated amount of HCl is dropped slowly into the solution. The dropping process has finished when the pH of solution is appropriate 5 and solution became transparent (called solution A). Similarly, solution B is prepared by using SnCl₂ salt instead of Zn(CH₃COO)₂.2H₂O. Solution A is used to deposit pure ZnO films. A mixture of solution A and solution B at a certain ratio is used to deposite SnO₂/ZnO films. The films were prepared by spraying the respective solutions onto a glass substrate at 400°C.

2.2. Characterization methods

The crystal structures are studied by X-ray diffractometer (D8 ADVANCE BRUCKER) with Cu K_{α} radiation ($\lambda=0.154056$ nm). Surface morphology is observed by SEM (HitachiS-4800). Optical properties are analyzed by UV-vis spectrophotometer (Jasco v-670). IV characteristics are performed by four-point probe method. The ethanol sensitivity is investigated by static method using a homemade system as showed in Figure 1. The resistance over time of the sample is measured using a Keithley 2000 multimeter interfaced with a computer. The sensor response is determined by R_a/R_g (where R_a and R_g are the resistances of the sample in air and in ethanol vapor, respectively). Ethanol is vaporized in the vaporization chamber at a specific concentration. The amount of ethanol vapor in the vaporization chamber is pumped into the measurement chamber. The ethanol concentration is calculated based on the ratio of the volume of ethanol vapor introduced into the measurement chamber to the volume of this chamber. To return the sample to its original state, clean air is pumped into the inlet, and ethanol vapor is extracted from the outlet of the measurement chamber. The computer records the entire process of resistance change to calculate the response of the sensor.

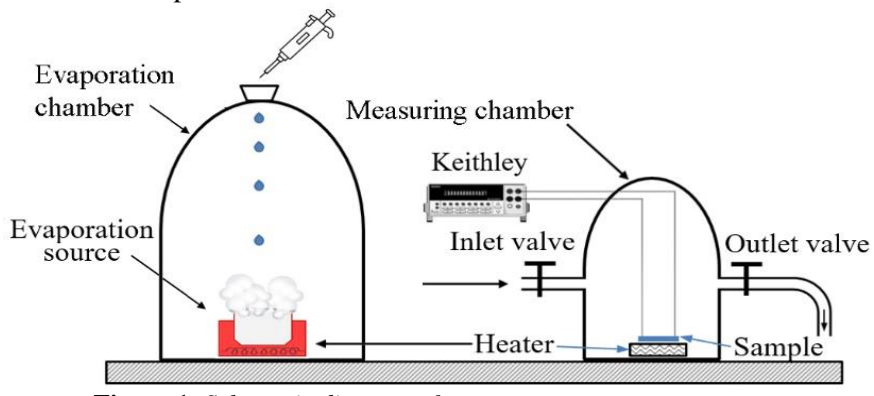


Figure 1. Schematic diagram of gas sensor measurement system

3. Results and discussion

Figure 2 shows the X-ray diffraction (XRD) patterns of SnO_2/ZnO thin films with different Sn/Zn ratios. For the pure ZnO films, the primary XRD peaks at 2θ angle positions of 34.364° , 47.469° and 62.754° correspond to the (002), (102) and (103) planes, which are consistent with the hexagonal Wurtzite crystal structure of ZnO (according to JCPDS card no. 36-1451). For composite films, revealing diffraction peaks indicative of mixed crystal oxide phases of ZnO, SnO_2 and SnO. The diffraction peaks associated with ZnO align well with the hexagonal Wurtzite crystal structure, similar to the pure ZnO films. In addition to the peaks of hexagonal Wurtzite ZnO structure, the remaining peaks at 2θ angle positions of 26.589° , 33.877° , 37.956° , and 51.777° correspond to the (110), (101), (200) and (211) planes of the standard tetragonal crystal structure of SnO_2 (according to JCPDS card no. 01-0657) and one peak at 2θ angle positions of 29.86° with very weak intensity of SnO (according to JCPDS card no. 01-072-1012). The number and intensity of SnO_2 diffraction peaks increase as the Sn/Zn ratio increases from 1/8 to 1/4. The absence of other diffraction peaks indicates no impurities. These confirmed that the SnO_2/ZnO composite films were successfully deposited.

The absorbance spectra of ZnO, SnO_2 , and composite SnO_2/ZnO films were analyzed within the wavelength range of 300-800 nm (Figure 3a) and their plots of $(\alpha hv)^2$ versus hv (Figure 3b). The absorption edge of the composite films is limited by the absorption edge of SnO_2 (corresponding to the wavelength of about 317 nm) and ZnO (corresponding to the wavelength of about 400 nm). The absorption edge of the composite film shifts toward the absorption edge of SnO_2 with the increase of the Sn/Zn ratio.

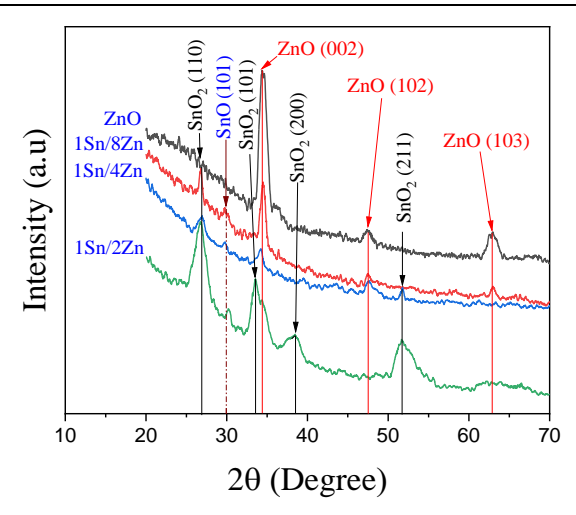


Figure 2. XRD pattern of ZnO and SnO₂/ZnO deposited on substrates with different Sn/Zn ratios

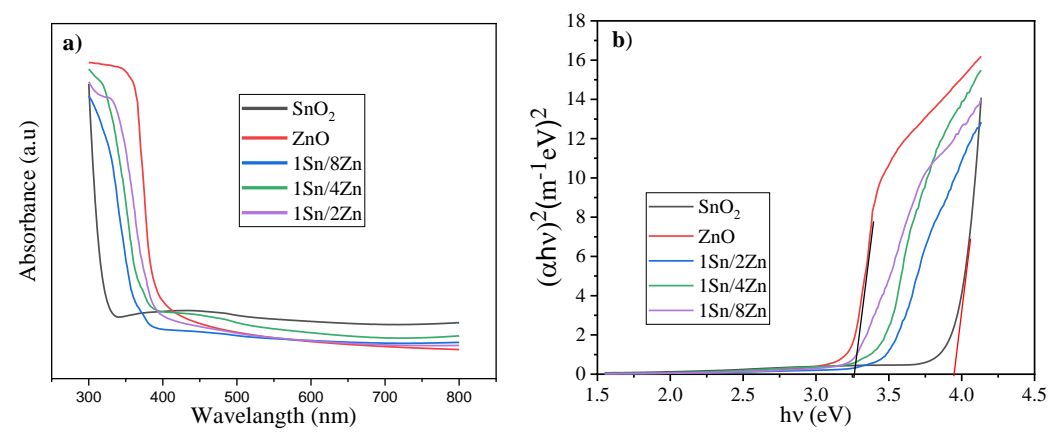
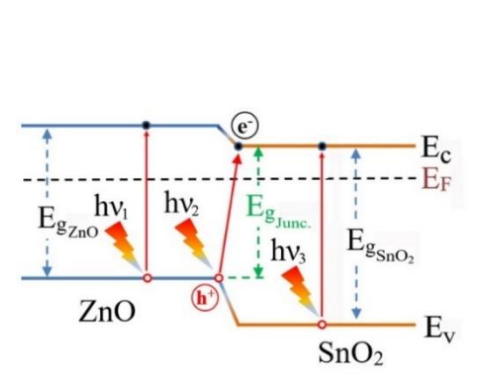


Figure 3. Optical properties of the SnO_2 and ZnO films: a) Absortion spectra of pure and composition films; b) plot of $(\alpha hv)^2$ vs. hv of pure and composition films

The results of calculating the band gap by the method of Tauc [29] show that the band gap of SnO_2 is about 3.94 eV and that of ZnO is 3.25 eV. This result is consistent with recent publications [6], [29] – [31]. The absorption mechanism of the composite film is quite complicated because it includes the absorption occurring inside the SnO_2 and ZnO particles and the absorption at the SnO_2/ZnO n-n heterojunction as shown in Figure 4 [11], [12], [14], [16]. The absorption at the heterojunction requires a smaller energy than that of both ZnO and SnO_2 . The absorption spectrum of the composite films is the mixture of all above absorption, so the absorption edge of the composite film lies between the absorption edges of the SnO_2 and SnO_2 films. In this case, Tauc's method should not be used to calculate the band gap, so the band gap of the composite film has not been mentioned.

Figure 5 is the I-V characteristic curve of ZnO film and SnO_2/ZnO film. The I-V curve of the ZnO film is fairly linear, with only a slight bending in the low voltage region. This bending is thought to be due to oxygen adsorption on the semiconductor surface, which creates a potential barrier at the grain boundaries. For the composite film, the I-V curve is distinctly nonlinear. This nonlinear curve indicates the formation of a heterojunction layer between the grain boundaries. The potential barrier in the heterojunction layer increases the film's resistance, reducing the slope of the I-V curve. Referring to the XRD results, it can predict that this heterojunction layer can only be the result of the contact between SnO_2 and ZnO.

The analyses of the crystal structure, electrical and optical properties have shown that the SnO₂/ZnO composite film has been successfully deposited.



40
30
30
20
1Sn/8Zn
1Sn/4Zn
10
-10
-20
-30
-40
-12 -10 -8 -6 -4 -2 0 2 4 6 8 10 12
V(V)

Figure 4. Schematic of ZnO–SnO₂ heterojunction

Figure 5. V-I characteristics of ZnO and SnO₂/ZnO composite films

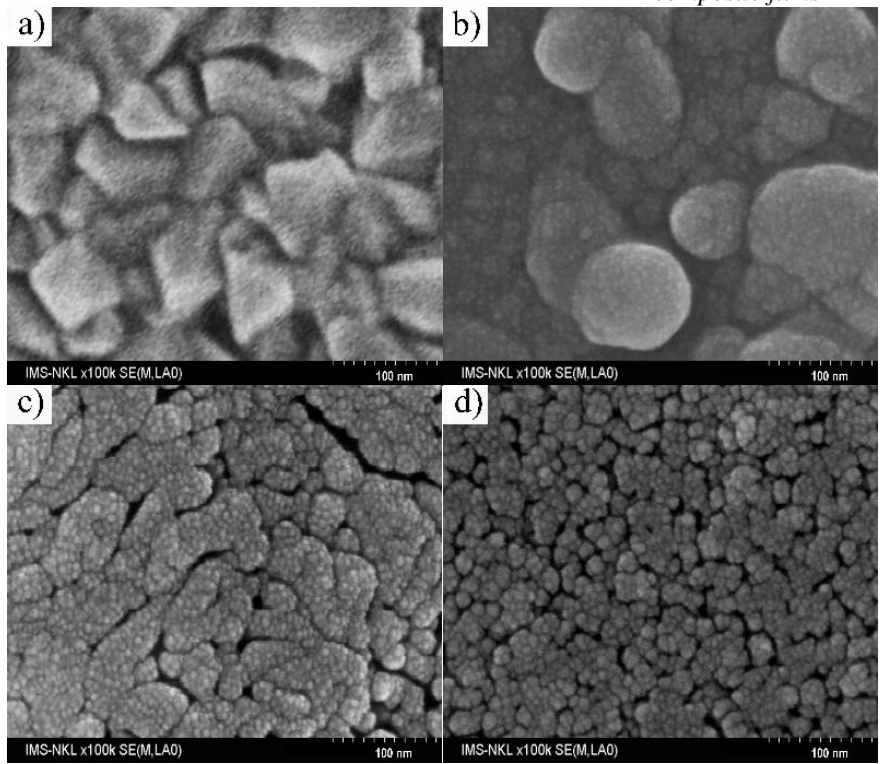


Figure 6. SEM images of SnO_2/ZnO films with different Sn/Zn ratios: a) ZnO, b) Sn/Zn=1/8, c) Sn/Zn=1/4, d) Sn/Zn=1/2

Figure 6 shows SEM images of SnO₂/ZnO films with different Sn/Zn ratios. For the pure ZnO films (Figure 6a), the main particles are hexagonal dipyramid crystals with an average size of about 50 nm. This reaffirms the formation of the hexagonal Wurtzite crystal structure of ZnO. When Sn is present at Sn/Zn ratio of 1/8 (Figure 6b), the crystal morphology is deformed. The sharp-edged pyramid-shaped crystals gradually transform into round grains with very small particles attached on their surfaces which are believed to be SnO₂. As the Sn/Zn ratio increases, the crystals become more strongly deformed. At an Sn/Zn ratio of 1/4, the particles appear as clusters with many small particles on their surfaces (Figure 6c). When the Sn/Zn ratio increases

to 1/2, the sample consists mainly of uniform particles around 10 nm in size that are bonded togethert to form a SnO_2/ZnO composite film (Figure 6d).

Temperature significantly affects the performance of sensors, particularly in gas detection applications. As temperature increases, the thermal energy supplied to the materials on the surface of sensor enhances gas reaction rates, thus improving the sensitivity and selectivity of sensor. However, excessively high temperatures can lead to reduced stability due to structural deformation and oxy absorption on the surface of sensors. Conversely, at low temperatures, surface reactions become less efficient, resulting in decreased sensitivity and slower response times. Therefore, optimizing the operating temperature is crucial for achieving the balancing sensitivity, response speed, and stability of sensors. In this study, the effect of temperature on the ethanol vapor sensitivity of SnO₂/ZnO films was evaluated at ethanol vapor concentration of 1000 ppm (Figure 7). The results indicate that both samples show negligible response to ethanol vapor at 150°C. The sensor response significantly increases when the operating temperature exceeds 200°C, the sensor response grows more slowly and tends to approach a saturation point. These findings are consistent with previous studies. For sensor applications, operating temperatures above this range offer limited benefits. Therefore, an operating temperature of 250°C was selected for further investigation.

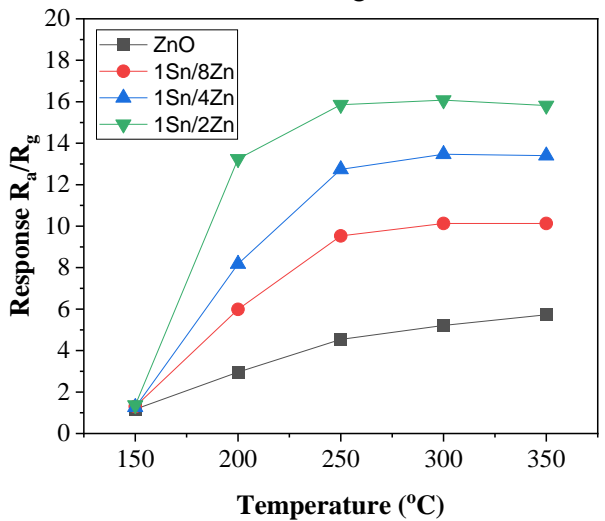


Figure 7. Influence of temperature on the sensor response of SnO₂/ZnO at ethanol concentration of 1000ppm

The effect of Sn/Zn ratios on the sensitivity of SnO₂/ZnO film-based sensors was investigated at an operating temperature of 250°C (Figure 8). The response and recovery times of the sensor to ethanol vapor, as shown in Figure 8a, indicate a rapid response to changes in the presence of ethanol vapor. Figure 8b illustrates the influence of Sn/Zn ratios on the sensor response to various ethanol vapor concentrations. The results demonstrate that the Sn/Zn ratio significantly affects the sensor response. Specifically, the sensor response increases with the increase of Sn/Zn ratios upto 1/2 at the same ethanol vapor concentration. Due to poor adhesion and excessive resistance of the film when the Sn/Zn ratio continued to increase, the ethanol vapor sensitivity of the film deposited with a Sn/Zn ratio greater than 1/2 was not further investigated.

When the SnO₂/ZnO film is exposed to air, it adsorbs oxygen molecules onto its surface, which capture free electrons from the conduction band, forming O₂-(ads). As the temperature increases, these adsorbed species transform into O⁻(ads) and O²-(ads), resulting in the formation of an electron depletion layer and increased material resistance due to electron loss. This process creates a barrier influenced by chemical and electron sensitization mechanisms. Besides, the work functions of SnO₂ (4.9 eV) is lower than that of ZnO (5.2 eV) and band gap of SnO₂ (3.6 eV) is higher than that of ZnO (3.37 eV) cause electrons transfer from SnO₂ to ZnO, leading to

the formation of depletion and accumulation layers, which generate a built-in electric field. This field increases the potential barrier and resistance. Furthermore, electron transport causes the work function to gradually decrease with increasing Sn concentration. A lower work function facilitates enhanced electron excitation, which holds significant potential for generating more absorbed oxygen and achieving improved gas sensing performance [11].

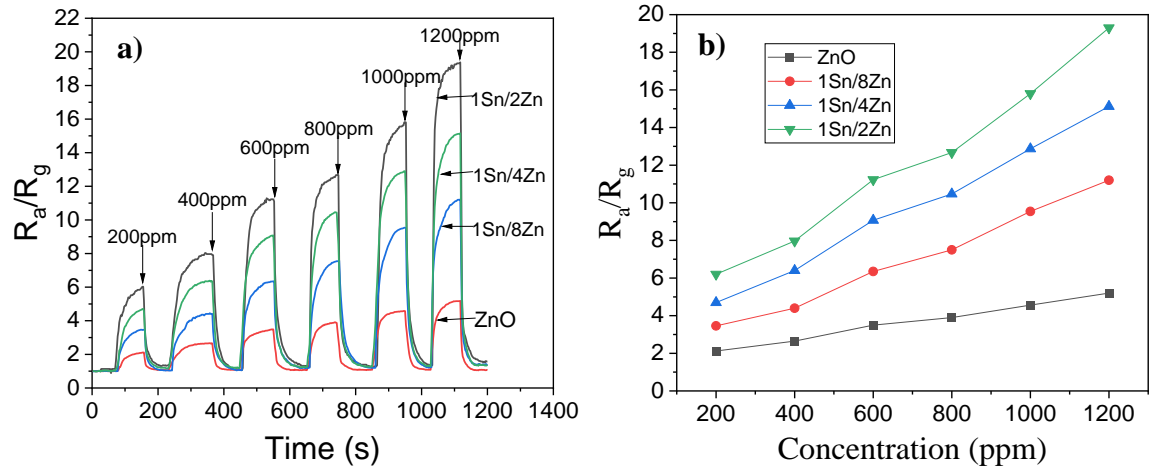


Figure 8. Influence of Sn/Zn ratios on the sensor response of the films at an operating temperature of 250°C: a) response and recovery time; b) sensor response versus ethanol vapor

When exposed to a reducing gas like ethanol, the adsorbed oxygen reacts with ethanol molecules, releasing captured electrons back to the conduction band, thus increasing electron concentration, reducing the barrier height, narrowing the depletion layer, and lowering material resistance [11], [13], [14], [16]. In addition to the above reasons, the surface morphology and grain size also play a very important role in improving the sensor sensitivity. The SEM image (Figure 6) shows that the film becomes uniform and the grain size decreases as the Sn/Zn ratio increases. This contributes to the improvement of the gas sensitivity of the film.

4. Conclusions

 SnO_2/ZnO nano composite films based ethanol sensor is deposited directly on glass substrate by a spray pyrolysis method at $400^{\circ}C$. The main crystalline phase structure are SnO_2 and ZnO. In addition, a small amount of SnO crystals still exists in the film. The number and intensity of SnO_2 diffraction peaks increase with the increase in the Sn/Zn ratio while their shape and size of the particles decrease. At a low Sn/Zn ratio, ZnO crystals have changed from pyramidal to round with small particles on the surface. When the Sn/Zn ratio reaches 1/2, the film structure consists of spherical particles about 10 nm in size interspersed with each other. Temperature significantly affects the ethanol vapor sensitivity of the film. The optimal sensitivity to ethanol vapor is achieved at $250^{\circ}C$. As the particle size decreases, the film response to ethanol also increases with the increase in the Sn/Zn ratio. The SnO_2/ZnO film with an Sn/Zn ratio of 1/2 exhibits the highest response to ethanol vapor.

REFERENCES

- [1] S. Popova, S. Lange, C. Probst, G. Gmel, and J. Rehm, "Estimation of national, regional, and global prevalence of ethanol use during pregnancy and fetal ethanol syndrome: a systematic review and meta-analysis," *The Lancet. Global Health*, vol. 5, no. 3, pp.e290-e299, 2017.
- [2] R. G. Jacob, G. K. Marilyn, N. Gery, P. Svetlana, H. Brandon, and B. Larry, "High prevalence of prenatal ethanol exposure detected by breathalyzer in the Republic of the Congo, Africa," *Neurotoxicology and Teratology*, vol. 80, 2020, Art. no. 106892.

- [3] R. V. B. Adriano, W. C. L. Rosamaria, and G. Jonas, "Polymeric electronic gas sensor for determining ethanol content in automotive fuels," *Sensors and Actuators B*, vol. 136, pp. 173-176, 2009.
- [4] L. Jonas, H. Bertil, A. Amin, and P. Håkan, "Passive in-vehicle driver breath ethanol detection using advanced sensor signal acquisition and fusion," *Traffic Injury Prevention*, vol.18, pp. S31-S36, 2017.
- [5] S. Paprocki, M. Qassem, and P. A. Kyriacou, "Review of Ethanol Intoxication Sensing Technologies and Techniques," *Sensors*, vol. 22, 2022, Art. no. 6819.
- [6] D. K. Chaudhary, T. R. Acharya, R. Shrestha, S. Gautam, P. Shrestha, A. Dhakal, S. P. Shrestha, A. A. Al-Khedhairy, R. Wahab, E. H. Choi, N. K. Kaushik, and L. P. Joshi, "Wide-range ethanol sensor based on a spray-deposited nanostructured ZnO and Sn-doped ZnO films," *Sensors and Actuators A: Physical*, vol. 370, 2024, Art. no. 115213.
- [7] D. Acharyya and P. Bhattacharyya, "Ethanol sensing performance of ZnO hexagonal nanotubes at low temperatures: A qualitative understanding," *Sensors and Actuators B: Chemical*, vol. 228, pp. 373-386, 2016.
- [8] C. S. Prajapati and P. P. Sahay, "Ethanol-sensing characteristics of spray deposited ZnO nano-particle thin films," *Sensors and Actuators B: Chemical*, vol. 160, pp. 1043-1049, 2011.
- [9] Y. Mingli, L. Mengdi, and L. Shengzhong, "Development of an ethanol sensor based on ZnO nanorods synthesized using a scalable solvothermal method," *Sensors and Actuators B: Chemical*, vol. 185, pp. 735-742, 2013.
- [10] B. J. Wang and S. Y. Ma, "High response ethanol gas sensor based on orthorhombic and tetragonal SnO₂," *Vacuum*, vol. 177, 2020, Art. no. 109428.
- [11] B. Jiang, T. Zhou, L. Zhang, J. Yang, W. Han, Y. Sun, F. Liu, P. Sun, H. Zhang, and G. Lu, "Separated detection of ethanol and acetone based on SnO₂-ZnO gas sensor with improved humidity tolerance," *Sensors & Actuators: B. Chemical*, vol. 393, 2023, Art. no. 134257.
- [12] S. Zhao, Y. Shen, P. Zhou, G. Li, F. Hao, C. Han, W. Liu, and D. Wei, "Construction of ZnO-SnO₂ n-n junction for dual-sensing of nitrogen dioxide and ethanol," *Vacuum*, vol. 181, 2020, Art. no. 109615.
- [13] J. Liu, T. Wang, B. Wang, P. Sun, Q. Yang, X. Liang, H. Song, and G. Lu, "Highly sensitive and low detection limit of ethanol gas sensor based on hollow SnO₂/ZnO spheres composite material," *Sensors and Actuators B*, vol. 245, pp. 551–559, 2017.
- [14] Z. M. Dong, Q. Xia, H. Ren, X. Shang, X. Lu, S. W. Joo, and J. Huang, "Preparation of hollow SnO2/ZnO cubes for the high-performance detection of VOCs," *Ceramics International*, vol. 49, pp. 4650-4658, 2023.
- [15] K. Du, L. Zhang, H. Shan, S. Dong, X. Shen, and G. Li, "Synthesis of ZnO nanorods loaded with SnO₂ cubes and the mechanism of improved ethanol sensing performance with DFT calculation," *Materials Science in Semiconductor Processing*, vol. 178, 2024, Art. no. 108429.
- [16] B. Mondal, B. Basumatari, J. Das, C. Roychaudhury, H. Saha, and N. Mukherjee, "ZnO–SnO₂ based composite type gas sensor for selective hydrogen sensing," *Sensors and Actuators B*, vol. 194, pp. 389-396, 2014.
- [17] B. Jiang, T. Zhou, L. Zhang, W. Han, J. Yang, C. Wang, Y. Sun, F. Liu, P. Sun, and G. Lu, "Construction of mesoporous In₂O₃-ZnO hierarchical structure gas sensor for ethanol detection," *Sensors & Actuators: B. Chemical*, vol. 393, 2023, Art. no. 134203.
- [18] T. Tharsika, A. S. M. A. Haseeb, and M. F. M. Sabri, "Structural and optical properties of ZnO–SnO₂ mixed thin films deposited by spray pyrolysis," *Thin Solid Films*, vol. 558, pp. 283-288, 2014.
- [19] A. I. Martinez and D. R. Acosta, "Effect of the fluorine content on the structural and electrical properties of SnO₂ and ZnO–SnO₂ thin films prepared by spray pyrolysis," *Thin Solid Films*, vol. 483, pp. 107-113, 2005.
- [20] W. Li, S. Ma, Y. Li, G. Yang, Y. Mao, J. Luo, D. Gengzang, X. Xu, and S. Yan, "Enhanced ethanol sensing performance of hollow ZnO–SnO₂ core–shell nanofibers," *Sensors and Actuators B*, vol. 211, pp. 392–402, 2015.
- [21] F. Atay, I. Akyuz, D. Durmaz, and S. Kose, "Characterization of ZnO-SnO₂ oxide systems produced by ultrasonic spray pyrolysis," *Solar Energy*, vol. 193, pp. 666-675, 2019.
- [22] L. Tao, P. Tang, J. Hu, and Y. Zhang, "The ethanol lock built on carbon-based feld-effect transistor sensor with Pd/ZnO floating gate structure used for drunk driving surveillance," *Sensors & Actuators: B. Chemical*, vol. 419, 2024, Art. no. 136393.
- [23] F. Gu, Y. Wang, D. Han, and Z. Wang, "Effects of ZnO crystal facet on the ethanol detection by the Au/ZnO sensors," *Talanta Open*, vol. 4, 2021, Art. no. 100068.

- [24] X. Y. Zhang, Q. Ren, C. Wang, L. Zhu, W. J. Ding, Y. Q. Cao, W. M. Li, D. Wu, and A. D. Li, "Atomic layer deposited SnO2/ZnO composite thin flm sensors with enhanced hydrogen sensing performance," *Applied Surface Science*, vol. 639, 2023, Art. no. 157973.
- [25] W. Ponhan, S. Phadungdhitidhada, and S. Choopun, "Fabrication of ethanol sensors based on ZnO thin film field-effect transistor prepared by thermal evaporation deposition," *Materials Today: Proceedings*, vol. 4, pp. 6342–6348, 2017.
- [26] A. Mhamdi, A. Labidi, B. Souissi, M. Kahlaoui, A. Yumak, K. Boubaker, A. Amlouk, and M. Amlouk, "Impedance spectroscopy and sensors under ethanol vapors application of sprayed vanadium-doped ZnO compounds," *Journal of Alloys and Compounds*, vol. 639, pp. 648–658, 2015.
- [27] X. Jia and H. Fan, "Preparation and ethanol sensing properties of the superstructure SnO₂/ZnO composite via ethanol-assisted hydrothermal route," *Materials Research Bulletin*, vol. 45, pp. 1496-1500, 2010.
- [28] H. A. Khorami, M. K. Rad, and M. R. Vaezi, "Synthesis of SnO₂/ZnO composite nanofibers by electrospinning method and study of its ethanol sensing properties," *Applied Surface Science*, vol. 257, pp. 7988-7992, 2011.
- [29] H. Zhonga, F. Panb, S. Yuec, C. Qine, V. Hadjievf, F. Tiang, X. Liuc, F. Linh, Z. Wangi, and J. Bao, "Idealizing Tauc Plot for Accurate Bandgap Determination of Semiconductor with Ultraviolet–Visible Spectroscopy: A Case Study for Cubic Boron Arsenide," *The Journal of Physical Chemistry Letters*, vol. 14, pp. 6702-6708, 2023.
- [30] W. Izydorczyk, K. Waczyski, J. Izydorczyk, P. Karasinski, J. Mazurkiewicz, M. Magnuski, J. Uljanow, N. W. Niemiec, and W. Filipowski, "Electrical and optical properties of spin-coated SnO₂ nanofilms," *Materials Science-Poland*, vol. 32, pp. 729-736, 2014.
- [31] A. S. Shamsipoor, M. M. B. Mohagheghi, and E. Mokaripoor, "Structural, electrical and optical properties of SnO₂: B transparent semiconducting thin films," *Progress in Physics of Applied Materials*, vol. 2, pp. 1-10, 2022.